High-speed optical coherence domain reflectometry

E. A. Swanson

Lincoln Laboratory, Massachusetts Institute of Technology, 244 Wood Street, Lexington, Massachusetts 02173-9108

D. Huang, M. R. Hee, and J. G. Fujimoto

Department of Electrical Engineering and Computer Science, Massachusetts Institute of Technology, Cambridge, Massachusetts 02139

C. P. Lin and C. A. Puliafito

Laser Research Laboratory, New England Eye Center, Tufts University School of Medicine, Boston, Massachusetts 02111

Received September 26, 1991

We describe a high-speed optical coherence domain reflectometer. Scan speeds of 40 mm/s are achieved with a dynamic range of >90 dB and a spatial resolution of 17 μm. Two applications are presented: the noninvasive measurement of anterior eye structure in a rabbit *in vivo* and the characterization of reflections and interelement spacing in a multielement lens.

Optical coherence domain reflectometry (OCDR) has emerged as an attractive method for obtaining high-spatial-resolution (<10 μm) reflectance measurements of fiber-optic, integrated-optic, and biological structures.[1-8] Most previous OCDR systems have achieved high sensitivity and dynamic range by using narrow-band heterodyne detection by piezoelectric path-length modulation and lock-in amplifier techniques. For many applications, present techniques are unacceptably slow. High speed is essential for applications to biological and medical diagnostics, where measurements must be performed rapidly compared with movement of a living subject. Speed is also important for process or assembly line diagnostics, as well as in any application that requires high data acquisition rates. By using a high-speed linear translation stage, OCDR measurements can be performed at high speeds with significant simplifications in system design. In this Letter we demonstrate a new OCDR technique for high-speed optical ranging measurements. Speeds approaching 40 mm/s with a dynamic range of >90 dB and a resolution of ~17 μm are achieved.

The basic schematic of the OCDR setup is shown in Fig. 1. A broadband light source such as a superluminescent diode (SLD) is coupled to a fiber-optic Michelson interferometer. One arm of the interferometer leads to the sample of interest, and the other leads to a reference mirror. Fiber-optic and integrated-optic samples can be directly attached to the sample arm fiber. For bulk-optical or biological samples, a probe module is used to direct the beam onto the sample and to collect the reflected signal. To aid in sample alignment, we use a fiber-coupled visible aiming laser. The reflected light beams are detected at the photodetector. They coherently interfere only when the sample and the reference path lengths are equal to within the source coherence length. Heterodyne detection is performed by taking advantage of the direct Doppler frequency shift that results from the uniform high-speed scan of the reference path length. Recording the interference signal magnitude as a function of the reference mirror position profiles the reflectance of the sample.

The spatial resolution, scan speed, and dynamic range of the OCDR system can be designed and optimized according to the desired application. If we assume a Gaussian line shape, the round-trip FWHM of the source intensity coherence envelope (ΔL) is related to the FWHM wavelength bandwidth ($\Delta\lambda$) of the source by

$$\Delta L = \ln(2)\frac{2}{\pi}\frac{\lambda^2}{\Delta\lambda}, \tag{1}$$

where λ is the optical wavelength. The Doppler frequency shift (f_D) that results from a uniform velocity scan (v) and the FWHM power bandwidth of the signal (Δf) are given by

$$f_D = 2\frac{v}{\lambda}, \tag{2}$$

$$\Delta f = \ln(4)\frac{4}{\pi}\frac{v}{\Delta L}. \tag{3}$$

The optimum bandwidth for the bandpass filter is approximately $2\Delta f$. Wider bandwidths will decrease sensitivity, whereas smaller bandwidths will decrease resolution.

Figure 2 shows the measured power spectral density of the light source (Laser Diode Model LDT-3201-SMF) and its FWHM value of 17.4 nm. Figure 3 show the measured interference signal at the photodetector and the demodulated envelope obtained by scanning the reference mirror at 37.5 mm/s. This speed was used in all the measurements reported here. Good agreement between the measured coherence envelope FWHM of 17.2 μm and the theoretical value of 16.7 μm [Eq. (1)] was

0146-9592/92/020151-03$5.00/0

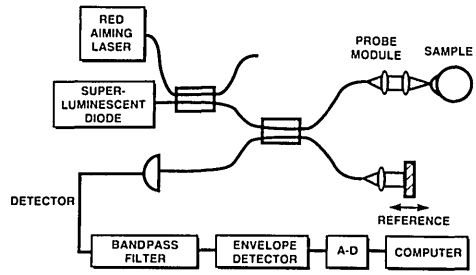

Fig. 1. Schematic of the high-speed OCDR system. A-D, analog-to-digital converter.

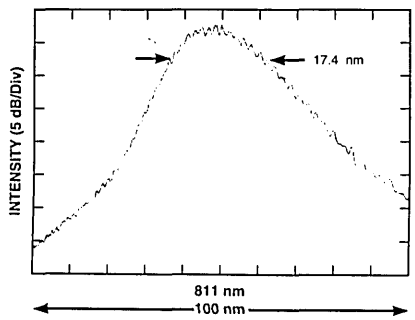

Fig. 2. SLD power spectral density.

obtained. The Doppler frequency shift was measured at ~93 kHz, also in good agreement with Eq. (2).

The approximate signal-to-noise ratio (SNR) in the bandpass filter if we assume shot-noise-limited detection is given by

$$\mathrm{SNR} = \frac{1}{2}\frac{\eta P_s}{h\nu}\frac{R_s}{\mathrm{NEB}}, \tag{4}$$

where η is the detector quantum efficiency, P_s is the sample signal power, h is Planck's constant, ν is the optical frequency, R_s is the sample reflectivity, and NEB is the noise-equivalent bandwidth of the bandpass filter. As stated above, NEB $\approx 2\Delta f$. Using Eq. (4) and assuming that a SNR = 2 is the limit of sensitivity, we can calculate the minimum resolvable reflectivity. Figure 4 shows the measured system sensitivity. A neutral-density 2.2 filter followed by a mirror was used to create a sample with a reflectivity of −44 dB. More than 90 dB of dynamic range is obtained at a power of 29.4 μW. The sidelobes are echoes that are due to imperfect antireflection coating in the SLD. Their location correlates well with the optical path length of the SLD. The filter NEB was 9.1 kHz, which is 2.3 times the signal FWHM of Δf = 3.9 kHz. With the above data and η = 0.8, the theoretical dynamic range is calculated to be 91 dB, indicating that the system has shot-noise-limited sensitivity.

OCDR provides a noncontact, high-sensitivity, high-resolution technique for optical ranging. High scan speeds are especially relevant for medical and biological diagnostic applications. One ophthalmologic problem of special interest is the noninvasive measurement of anterior eye dimensions. Measurements of corneal thickness or incision depth are useful for keratorefractive surgeries[9], while measurements of anterior chamber depth are useful in determining the refractive power of intraocular lens implants[10] as well as in the diagnosis of angle-closure glaucoma.[11] Although ultrasound ranging has been used extensively in ophthalmology,[12] it requires direct physical contact of the eye by an ultrasound transducer or saline immersion of the eye in order to facilitate the transmission of acoustic waves into the eye. In contrast, OCDR is a noncontact diagnostic.

In order to demonstrate the clinical potential of high-speed OCDR, measurements of eye structure were performed in an anesthetized Dutch pigmented rabbit *in vivo*. Figures 5(a) and 5(b) show an OCDR measurement of the anterior eye along with a sketch of rabbit eye structure for comparison.[13] The output from the sample fiber was collimated with a 20-mm focal-length lens and subsequently focused into the anterior eye by using a 150-mm focal-length lens. The depth of field was measured to be ~3 mm FWHM. The scan speed was 37.5 mm/s, and the scan range was 7.5 mm. Reflection peaks at the air–cornea, cornea–aqueous, and aqueous–lens interfaces as well as scattering from within the cornea can be seen. An echo of the air–cornea interface is also visible. It results from the imperfect SLD facet coating mentioned above. The refractive indices of the cornea (n = 1.376) and the aqueous (n = 1.336) (Ref. 13) were used to determine the measured cornea thickness of 396 μm and the anterior chamber depth of 2.40 mm. The optical power incident on the sample eye was 29.4 μW, far below the Ameri-

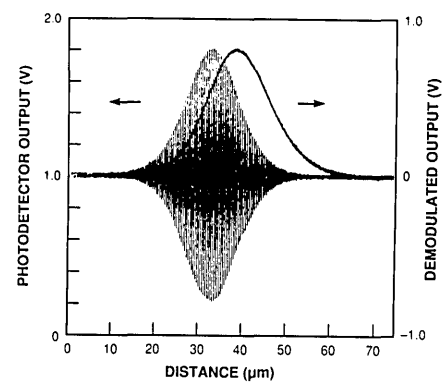

Fig. 3. Interference signal at the photodector and demodulated interference envelope.

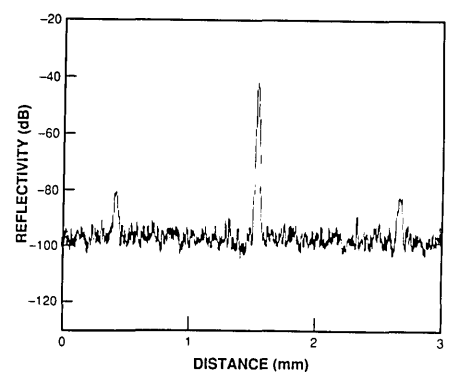

Fig. 4. System sensitivity.

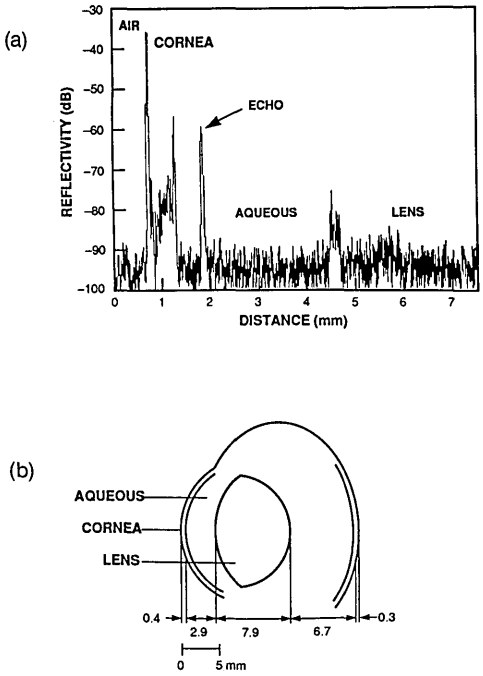

Fig. 5. (a) Measurement of the anterior of a rabbit eye performed *in vivo*. (b) Schematic of eye structure.

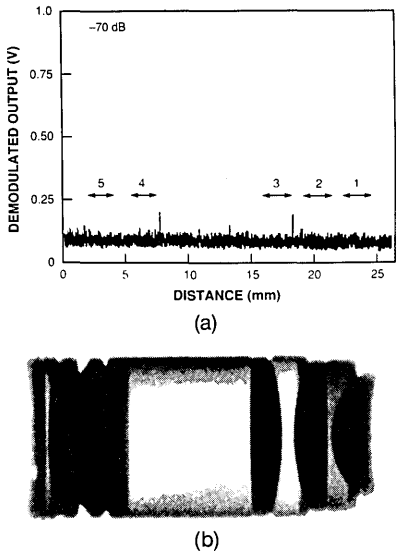

Fig. 6. (a) Measurement of multielement laser-diode collimating lens. (b) An x ray of the lens.

can National Standards Institute safe ocular exposure standard of 200 μW at 830 nm.

In addition to diagnostics in biological systems, high-speed OCDR has numerous applications for noncontact diagnostics of precision mechanical and optical systems as well as for process control and monitoring in manufacturing. One example is the testing of optical components. We investigated the feedback characteristics of a commercially available multielement laser-diode collimating lens (Fujinon LSR-35B) using high-speed OCDR scanning. Diagnostics of multielement collimating lenses are important because semiconductor laser diodes are known to be sensitive to feedback. In addition, OCDR provides a direct measurement of interelement distances in the lens assembly. The Fujinon lens was used to collimate the light output from the sample arm. Figures 6(a) and 6(b) show the measured reflectance profile along with an x ray of the lens. The lens has five elements and an optical path length of approximately 23 mm. The maximum scan length of the reference mirror is 20 mm. Figure 6(a) was constructed by using a composite of two scans. The spacing between lenses, the lens thickness, and the reflection coefficients of the various interfaces can be seen. Although the reflection amplitudes are sensitive to alignment, a maximum feedback of approximately −70 dB arises from the last surface of the last lens.

In summary, we have demonstrated an OCDR system that achieves high-speed, high-sensitivity, and high-resolution measurements by performing heterodyne detection at the Doppler frequency shift that results from the high-speed scan. This new technique makes possible a variety of new OCDR applications, including diagnostics in medicine and biological systems and the precision monitoring of mechanical systems in process control and manufacturing.

We thank J. S. Schuman, W. G. Stinson, T. F. Deutsch, and R. Birngruber for helpful comments and suggestions. This research was supported by National Institutes of Health grant RO1-GM35459-06, U.S. Office of Naval Research Medical Free Electron Laser Program grant N00014-91-C-0084, the Johnson and Johnson Foundation, and the U.S. Department of the Air Force.

References

1. R. C. Youngquist, S. Carr, and D. E. N. Davies, Opt. Lett. **12,** 158 (1987).
2. K. Takada, I. Yokohama, K. Chida, and J. Noda, Appl. Opt. **26,** 1063 (1987).
3. D. Huang, J. Wang, J. G. Fujimoto, C. P. Lin, and C. A. Puliafito, in *Digest of Conference on Lasers and Electro-Optics* (Optical Society of America, Washington, D.C., 1990), paper CFK1.
4. R. P. Novak and H. H. Gilgen, in *Symposium on Optical Fiber Measurements* (National Institute of Standards and Technology, Boulder, Colo., 1990), paper PB91-13208.
5. C. K. Hitzenberger, Invest. Ophthalmol. Vis. Sci. **32,** 616 (1991).
6. E. A. Swanson, D. Huang, J. G. Fujimoto, C. P. Lin, and C. A. Puliafito, in *Digest of Conference on Lasers and Electro-Optics* (Optical Society of America, Washington, D.C., 1991), paper CTuS2.
7. M. Kobayashi, H. Hanafasu, K. Takada, and J. Noda, IEEE J. Lightwave Technol. **9,** 623 (1991).
8. M. Kobayashi, H. F. Taylor, K. Takada, and J. Noda, IEEE Photon. Technol. Lett. **3,** 564 (1991).
9. A. Hughes, Vis. Res. **12,** 123 (1976).
10. H. J. F. Schammas, Am. Intra-Ocular Implant Soc. J. **8,** 346 (1982).
11. M. B. Shields, *Textbook of Glaucoma,* 2nd ed. (Williams and Wilkins, Baltimore, Md., 1987), Chap. 9.
12. S. P. Thornton, Ophthalmic Surg. **15,** 933 (1984).
13. V. B. Mountcastle, ed., *Medical Physiology,* 14th ed. (Mosby, St. Louis, Mo., 1980).